

# Fatigue life prediction of complex 2D components under mixed-mode variable amplitude loading

Antonio Carlos de Oliveira Miranda <sup>a</sup>, Marco Antonio Meggiolaro <sup>b</sup>,  
Jaime Tupiassú Pinho de Castro <sup>b,\*</sup>, Luiz Fernando Martha <sup>a</sup>

<sup>a</sup> Department of Civil Engineering, Pontifical Catholic University of Rio de Janeiro, Rua Marquês de São Vicente 225 – Gávea, Rio de Janeiro, RJ 22453-900, Brazil

<sup>b</sup> Department of Mechanical Engineering, Pontifical Catholic University of Rio de Janeiro, Rua Marquês de São Vicente 225 – Gávea, Rio de Janeiro, RJ 22453-900, Brazil

## Abstract

Accurate residual fatigue life predictions under variable amplitude (VA) loading are essential to maximize the time between the required inspections in defect-tolerant structures. However, this is not a trivial task for real structural components, in which cracks may change direction as they grow due to mixed-mode loading. Such curved crack paths can be predicted using finite element (FE) techniques, but this approach is not computationally efficient to predict the residual life, because it would require time-consuming remeshing of the entire structure after each rain-flow counted load event under VA loading. In this work, a two-phase methodology that is both precise and cost-effective is applied to solve this problem. First, the fatigue crack path and stress intensity factors  $K_I$  and  $K_{II}$  are calculated in a specialized (global) FE program using fixed crack increments, requiring only relatively few remeshing steps. Then, an analytical expression is fitted to the calculated  $K_I(a)$  values, where  $a$  is the length along the crack path, and exported to a companion fatigue design program to predict the crack propagation life by the local approach, considering load interaction effects such as crack retardation or arrest after overloads. This two-phase methodology is experimentally validated by fatigue tests on compact tension specimens, modified with holes positioned to attract or to deflect the cracks.

© 2003 Elsevier Ltd. All rights reserved.

**Keywords:** Fatigue crack growth; Curved cracks; Finite elements; Load interaction effects

## 1. Introduction

Fatigue life prediction under variable amplitude (VA) loading in complex two-dimensional (2D) structural components is a challenging problem that requires the calculation of the generally curved crack path, the associated stress intensity factors (SIF), and the crack propagation rate at each load step. Due to its versatility, a finite element (FE) global discretization of the component using an appropriate mesh with specialized crack tip elements is a standard design practice to predict the crack path and to calculate its associated SIF  $K_I$  and  $K_{II}$ . It can also be very efficient under constant amplitude

(CA) loading, if appropriate automatic remeshing procedures are included in the FE code.

However, this global method is not computationally efficient to predict fatigue lives under VA loading, because it would require time-consuming remeshing procedures and FE recalculations of the entire structure stress/strain field after each load event counted by the sequential rain-flow method. Moreover, the FE modeling of crack retardation effects is, at best, only a partially solved problem, and still cannot be reliably used in practical fatigue life predictions under VA loading.

On the other hand, the local approach, based on the direct integration of the crack propagation equation, can be efficiently used to calculate the crack increment at each VA load event, considering crack growth retardation or acceleration effects using semi-empirical design rules. However, this approach requires the stress intensity expression for the crack, which is simply not available for most real components. In these cases, the

\* Corresponding author. Tel.: +55-21-2511-5846; fax: +55-21-3114-1165.

E-mail addresses: [amiranda@tecgraf.puc-rio.br](mailto:amiranda@tecgraf.puc-rio.br) (A.C. de Oliveira Miranda); [meggi@mec.puc-rio.br](mailto:meggi@mec.puc-rio.br) (M.A. Meggiolaro); [jtcastro@mec.puc-rio.br](mailto:jtcastro@mec.puc-rio.br) (J.T.P. de Castro); [lfm@civ.puc-rio.br](mailto:lfm@civ.puc-rio.br) (L.F. Martha).

errors involved in using approximate  $K_I$  handbook expressions increase as the real crack deviates from the tabulated one, making the local approach accuracy questionable.

Since the advantages of the two approaches are complementary, the problem can be successfully divided into two steps [1]. First, the (generally curved) fatigue crack path and its SIF are calculated in a specialized FE program, using pre-fixed small crack increments and automatic mesh generation schemes. Specialized numerical methods are used to calculate the crack propagation path, based on the computation of the crack incremental direction, and the SIF  $K_I$  and  $K_{II}$  generated by the FE program. Then, an analytical expression is fitted to the associated mode I SIF  $K_I(a)$ , where  $a$  is the length along the crack path. This  $K_I(a)$  expression is used as an input to a general purpose fatigue design program based on the local approach, where the actual VA loading is efficiently treated by the integration of the crack propagation equation, considering load interaction effects if required.

This methodology has been experimentally validated through crack growth under CA loading experiments on modified compact tension C(T) specimens, in which holes were machined to curve the crack propagation path [2]. In this work, the methodology is extended to VA loading cases, considering load interaction effects. Several crack retardation models were calibrated by testing regular C(T) specimens under VA loading, and the calibrated parameters were used to predict the fatigue lives of the modified C(T) specimens under similar conditions. In the next section, the methods used to calculate the SIF in arbitrary 2D FE models are reviewed.

## 2. Numerical computation of stress-intensity factors

At least three methods can be chosen to compute the SIF along the (generally curved) crack path under mixed mode I–mode II loading: (i) the displacement correlation technique [3], (ii) the potential energy release rate computed by means of a modified crack-closure integral technique [4,5], and (iii) the  $J$ -integral computed by means of the equivalent domain integral (EDI) together with a mode decomposition scheme [6,7]. Since Bitencourt et al. [8] showed that for sufficiently refined FE meshes all three methods predict essentially the same results, only the EDI method is summarized below.

The  $J$ -integral is a path independent contour integral introduced by Rice [9] to study non-linear elastic materials under small scale yielding. The EDI method replaces the  $J$ -integral along a contour around the crack tip by another one over a finite size domain that is more convenient for FE analysis, using the divergence theorem. For 2D problems, the  $J$ -integral is written as an area integral:

$$J = - \int_A \left[ W \frac{\partial q}{\partial x} - \sigma_{ij} \frac{\partial u_i \partial q}{\partial x \partial x} \right] dA - \int_A \left\{ \frac{\partial W}{\partial x} - \frac{\partial}{\partial x} \left[ \sigma_{ij} \frac{\partial u_i}{\partial x} \right] \right\} q dA - \int_s t_i \frac{\partial u_i}{\partial x} q ds \quad (1)$$

where  $W$  is the strain energy density;  $q$  is a continuous function allowing the EDI to be used in FE formulations;  $\sigma_{ij}$  are the stresses;  $u_i$  are the displacements correspondent to local  $i$ -axes;  $t_i$  is the crack face load; and  $s$  is the contour arc-length. Usually, a linear function is chosen for  $q$ , which assumes a unit value at the crack tip and a null value along the contour. For the special case of linear-elastic materials, the second term in Eq. (1) vanishes. The third term will vanish if the crack faces are not loaded, or if  $q = 0$  at its loaded portions.

The  $J$ -integral definition considers a balance of mechanical energy for a virtual translation field along the  $x$ -axis. In the case of either pure Mode I or pure Mode II, Eq. (1) allows for the calculation of  $K_I$  or  $K_{II}$ . However, in the mixed-mode case,  $K_I$  and  $K_{II}$  cannot be calculated separately from this equation alone. In this case, other invariant integrals are used. Usually, the expression defined by Knowles and Sternberg [10] is adopted:

$$J_k = - \int_A \left[ W \frac{\partial q}{\partial x_k} - \sigma_{ij} \frac{\partial u_i \partial q}{\partial x_k \partial x_j} \right] dA - \int_A \left[ \frac{\partial W}{\partial x_k} - \sigma_{ij} \frac{\partial}{\partial x_j} \left( \frac{\partial u_i}{\partial x_k} \right) \right] q dA - \int_s t_i \frac{\partial u_i}{\partial x_k} q ds \quad (2)$$

where  $k$  is an index for local crack tip axes ( $x, y$ ). These integrals were introduced initially for very small deformations [9] and were extended by Atluri [11] for finite deformations. The integration is performed in the elements chosen to represent the domain. In the Quebra2D program used in this work, the chosen domain is the rosette of quarter-point elements at the crack tip, and the Gaussian quadrature is used over each element [1,2].

For linear elastic problems, Bui [12] proposed associated fields to decompose the loading modes. In this case, the first component in Eq. (2) is path independent, but the second one is not. However, the path dependency may be eliminated if the displacements and the stress fields are decomposed into symmetric and anti-symmetric portions, rewriting the displacement field as:

$$u = u^I + u^{II} = \frac{1}{2}(u + u') + \frac{1}{2}(u - u') \quad \text{and} \quad (3)$$

$$v = v^I + v^{II} = \frac{1}{2}(v - v') + \frac{1}{2}(v + v')$$

where  $u$  and  $v$  are displacements in  $x$  and  $y$  directions;  $u'(x,y) \equiv u'(x,-y)$  and  $v'(x,y) \equiv v'(x,-y)$ ; and the superscript I and II correspond to the symmetric (Mode I) and anti-symmetric (Mode II) components of the displacement field, respectively. New integrals  $J_I$  and  $J_{II}$  are

obtained, which satisfy the condition  $J = J_I + J_{II}$ , where  $J_I$  is associated to Mode I and  $J_{II}$  to Mode II:

$$J_{I,II} = - \int_A \left[ W(u_i^{I,II}) \frac{\partial q}{\partial x_k} - \sigma_{ij}(u_i^{I,II}) \frac{\partial u_j^{I,II}}{\partial x_k} \frac{\partial q}{\partial x_j} \right] dA \quad (4)$$

$$- \int_S t_i \frac{\partial u_i^{I,II}}{\partial x_k} q ds$$

This approach has also been applied by Atluri [11] with highly accurate results for mixed-mode problems. These modifications and decomposition techniques allow for the use of the  $J$ -integral and EDI approaches for a wide range of linear and non-linear deformation crack problems. Also, under linear elastic conditions (LEFM),  $J$  is equal to the energy release rate  $G$ , and its components  $J_I$  and  $J_{II}$  may be used to compute SIF  $K_I$  and  $K_{II}$  by means of:

$$G_I = \frac{\kappa + 1}{8\mu} K_I^2 \text{ and } G_{II} = \frac{\kappa + 1}{8\mu} K_{II}^2 \quad (5)$$

where  $\kappa = 3 - 4\nu$  for plane strain,  $\kappa = (3 - \nu)/(1 + \nu)$  for plane stress,  $\nu$  is the Poisson ratio, and  $\mu$  is the shear modulus.

### 3. Numerical computation of the crack increment direction

In 2D FE analysis, the three most used criteria for numerical computation of crack incremental growth direction in the linear-elastic regime are: (i) the maximum circumferential stress ( $\sigma_{\theta_{\max}}$ ), (ii) the maximum potential energy release rate ( $G_{\theta_{\max}}$ ), and (iii) the minimum strain energy density ( $U_{\theta_{\min}}$ ) [1,2].

In the first criterion, Erdogan and Sih [13] considered that the crack extension should occur in the direction that maximizes the circumferential stress in the region close to the crack tip. In the second, Hussain et al. [14] have suggested that the crack extension occurs in the direction that causes the maximum fracturing energy release rate. And in the last criterion, Sih [15] assumed that the crack growth direction is determined by the minimum strain energy density value near the crack tip. Bittencourt et al. [8] have shown that if the crack orientation is allowed to change in automatic simulation, the three criteria provide basically the same results. Since the  $\sigma_{\theta_{\max}}$  criterion is the simplest, even presenting a closed form solution, it is described below.

First, the stresses obtained from the global finite-element analysis are transformed to a local system at the crack tip. Then, the maximum circumferential stress criterion determines that crack extension begins on a plane perpendicular to the direction in which the circumferential stress  $\sigma_{\theta}$  is maximum (in polar coordinates). The angle  $\theta$  between the crack extension and the crack front planes is then obtained under mixed-mode:

$$\theta = 2 \arctan \left( \frac{1}{4} \frac{K_I}{K_{II}} \pm \frac{1}{4} \sqrt{\left( \frac{K_I}{K_{II}} \right)^2 + 8} \right) \quad (6)$$

where  $K_I$  and  $K_{II}$  are the Mode I and II SIF, and the sign of  $\theta$  is the opposite of the sign of  $K_{II}$ .

The Quebra2D program used in this work allows the user to choose the SIF calculation method and the crack incremental direction criterion. In this work, all predictions were made using the EDI method to calculate  $K_I(a)$  and the  $\sigma_{\theta_{\max}}$  criterion to obtain the crack path.

### 4. Load interaction models

Load cycle interactions can have a very significant effect on the prediction of residual fatigue life. Normally, tensile overloads can retard or arrest the subsequent crack growth, and compressive underloads can accelerate it [16–21]. Neglecting these sequence effects in fatigue life calculations can completely invalidate the predictions. However, the generation of a universal algorithm to quantify these sequence effects in fatigue crack growth (FCG) is particularly difficult, due to the number and to the complexity of the mechanisms involved, such as plasticity-induced crack closure, blunting and/or bifurcation of the crack tip, residual stresses and strains, incompatible crack front orientation, strain-hardening, crack face roughness, and oxidation of the crack faces, e.g. besides, depending on the case, several of these mechanisms may act concomitantly or competitively, as a function of factors such as crack size, material microstructure, dominant stress-state, and environment.

Elber's plasticity-induced crack closure [22], which is generated by the plastic wake that surrounds the crack faces as schematically shown in Fig. 1, has long been used to satisfactorily explain the phenomenology of plane-stress load interaction effects [23]. According to Elber, only after completely opening the crack at a load  $K_{op}$  would the crack tip be stressed. Therefore, the bigger the  $K_{op}$ , the less would be the effective stress intensity range  $\Delta K_{\text{eff}} = K_{\max} - K_{op}$ , and this  $\Delta K_{\text{eff}}$  instead of  $\Delta K$  would be the crack propagation rate controlling parameter. Based on this assumption, Elber proposed a modification to the Paris FCG equation taking into account the crack closure concept:

$$\frac{da}{dN} = A \cdot (K_{\max} - K_{op})^m = A \cdot (\Delta K_{\text{eff}})^m \quad (7)$$

where  $A$  and  $m$  are material constants, which should be experimentally measured. The Elber mechanism can be used to justify the experimentally observed FCG retardation after tensile overloads (OL) by the increase they cause in the crack closure level. Neglecting crack closure in fatigue life calculations under VA loadings can result in overly conservative predictions, increasing mainte-

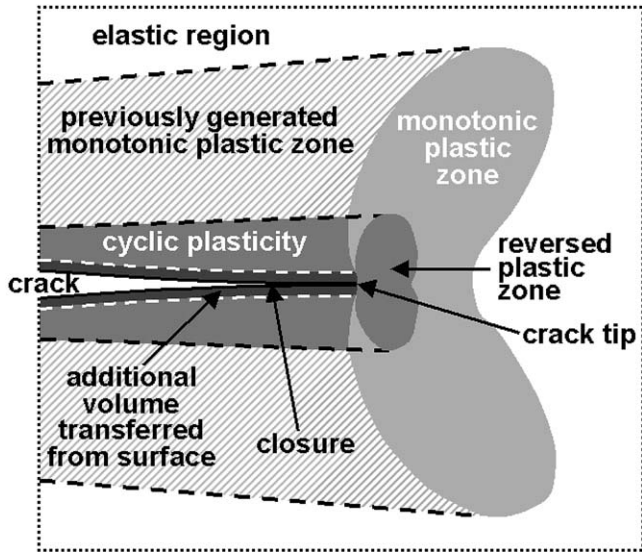


Fig. 1. Schematic of plasticity-induced crack closure, showing the residual deformation left in the crack wake by the monotonic and reversed plastic zones.

nance costs by unnecessarily reducing the period between inspections.

Several models have been developed to account for load sequence interaction effects in FCG based on OL-induced changes in the fatigue crack plastic envelope. These methods can be subdivided into three main categories [24]: (i) yield zone models, which account for retardation by comparing the OL and the current plastic zone sizes,  $Z_{ol}$  and  $Z_i$  in Fig. 2 (which could capture retardation caused by either crack closure or residual stress fields); (ii) crack closure models, which estimate the crack opening loads from experimental data; and (iii) strip-yield models, which numerically calculate the crack closure relations based on Dugdale’s model [25].

Perhaps the best-known yield zone models are those developed by Wheeler [26] and by Willenborg et al. [27]. Both use the same idea to decide whether the crack growth is retarded or not: under VA loading, FCG retardation is predicted when the plastic zone of the  $i$ -th load event  $Z_i$  after an OL is embedded within the plastic zone  $Z_{ol}$  induced by that (previous) OL, and the amount of retardation (as compared to the FCG rate that would be obtained at the  $i$ -th load cycle if the OL had no effect) is assumed dependent on the distance from the border

of  $Z_{ol}$  to the tip of the  $i$ -th crack plastic zone  $Z_i$ , see Fig. 2.

The Wheeler model introduces a crack-growth reduction factor bounded by zero and unity. This factor is calculated for each load cycle after the OL to predict retardation as long as the current plastic zone  $Z_i$  is contained within a previously OL-induced plastic zone  $Z_{ol}$ . The retardation is maximum just after the OL (therefore it neglects delayed retardation effects), and stops when the border of  $Z_i$  touches the border of  $Z_{ol}$  (Fig. 2).

Thus, if  $a_{ol}$  and  $a_i$  are the crack sizes at the instant of the OL and at the (later)  $i$ -th cycle, and  $(da/dN)_{ret,i}$  and  $(da/dN)_i$  are the retarded crack growth rate and the corresponding non-retarded rate (at which the crack would be growing in the  $i$ -th cycle if the OL had not occurred), then, according to Wheeler

$$\left(\frac{da}{dN}\right)_{ret,i} = \left(\frac{da}{dN}\right)_i \cdot \left(\frac{Z_i}{Z_{ol} + a_{ol} - a_i}\right)^\beta, \tag{8}$$

$$a_i + Z_i < a_{ol} + Z_{ol}$$

where  $\beta$  is an experimentally adjustable constant.

However, this model cannot predict OL-induced crack arrest because the resulting  $(da/dN)_{ret,i}$  is always positive. Cut-off values have been proposed to include crack arrest in the original Wheeler model, however this approach results in discontinuous  $da/dN$  equations. A simple but effective modification to the original Wheeler model can be used to predict both crack retardation and arrest in a continuous way. This approach, called the Modified Wheeler model [21], uses a Wheeler-like parameter to multiply  $\Delta K$  instead of  $da/dN$  after the OL:

$$\Delta K_{ret}(a_i) = \Delta K(a_i) \cdot \left(\frac{Z_i}{Z_{ol} + a_{ol} - a_i}\right)^\gamma, \tag{9}$$

$$a_i + Z_i < a_{ol} + Z_{ol}$$

where  $\Delta K_{ret}(a_i)$  and  $\Delta K(a_i)$  are the values of the stress intensity ranges that would be acting at  $a_i$  with and without retardation due to the OL, and  $\gamma$  is an experimentally adjustable constant, in general different from the original Wheeler model exponent  $\beta$ . This simple modification can be used with any of the crack propagation equations that recognize  $\Delta K_{th}$  to predict both retardation and arrest of fatigue cracks after an OL, the arrest occurring if  $\Delta K_{ret}(a_i) \leq \Delta K_{th}$ .

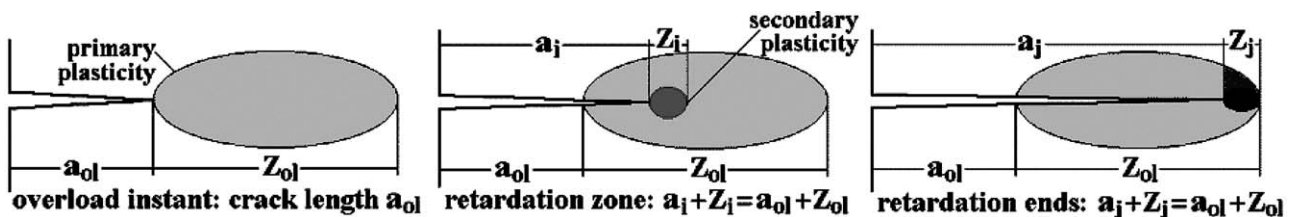


Fig. 2. Yield zone crack growth retardation region used by the Wheeler and Willenborg load interaction models ( $Z_{ol}$  is the OL and  $Z_i$  is the  $i$ -th cycle plastic zone sizes).

Another yield zone model was proposed by Willenborg et al. [27], who assumed that the maximum SIF  $K_{\max}$  occurring at the current crack length  $a_i$  is reduced by a residual stress intensity  $K_{RW}$ , calculated, more or less arbitrarily, from the difference between the stress intensity required to produce a plastic zone that would reach the OL zone border (distant  $Z_{oi}+a_{oi}-a_i$  from the current crack tip) and the current maximum applied stress intensity  $K_{\max}$ . Willenborg assumed that both  $K_{\max}$  and  $K_{\min}$  at the current  $i$ -th cycle are reduced by  $K_{RW}$ . Thus, since the stress intensity range  $\Delta K$  is unchanged by this uniform reduction, the retardation effect is only caused by the change in the effective load ratio  $R_{\text{eff}}$ . An important drawback in the original Willenborg model is the prediction of crack arrest immediately after a 100% overload, independently of the material properties, stress level, or load spectrum. Several modifications have been proposed to improve the original model, however the assumption regarding the accounting of OL-induced residual compressive stresses through  $K_{RW}$  is at least very doubtful.

Among the crack closure models, probably the simplest one is the Constant Closure model, originally developed at Northrop for use on their classified programs [28]. This load interaction model is based on the observation that for some flight load spectra the closure stresses did not deviate significantly from a certain stabilized value, which was then assumed to be constant. The opening load  $K_{op}$  used in VA FCG calculations is generally estimated between 20% and 50% of the maximum OL, or  $0.2K_{ol,\max} < K_{op} < 0.5K_{ol,\max}$ , where  $K_{ol,\max}$  is the load spectrum peak. These peaks must occur frequently and more or less well distributed along the load history, i.e. this stabilized closure value is determined by assuming that the spectrum has both a “controlling overload” and a “controlling underload” that occur often enough to keep the closure level constant.

The main limitation of the Constant Closure model is that it can only be applied to loading histories with “frequent controlling overloads,” because it does not model the decreasing retardation effects experimentally observed as the crack tip cuts through a single OL plastic zone [18]. In other words, by keeping  $K_{op}$  constant, this model assumes that a new overload plastic zone, with primary plasticity (Fig. 2), is formed often enough to act before the crack can significantly propagate through the previous OL-induced plastic zone, and that secondary plasticity effects can be neglected in the intervals between OLs.

Other crack closure models have been proposed to predict the influence of the load ratio  $R=K_{\min}/K_{\max}$  on  $K_{op}$ , such as the one proposed by Schijve [29]:

$$K_{op}/K_{\max} = 0.45 + (0.1 + \lambda) \cdot R + (0.45 - 2\lambda) \cdot R^2 + \lambda \cdot R^3 \quad (10)$$

where  $\lambda$  is a material dependent constant, equal to 0.1 for a 2024-T3 Alclad aluminum alloy.

Newman [30] concluded from FE calculations that crack closure depends not only on the load ratio  $R$ , but also on the ratio between the maximum stress level  $\sigma_{\max}$  and the material flow strength  $S_{fl}$  (defined as the average between the material yielding and ultimate strengths), and on a stress-state (plane stress/plane strain) constraint factor  $\alpha$ . This stress-state constraint typically ranges from  $\alpha = 1$  for pure plane-stress (but a value  $\alpha = 1.15$  has a better agreement with experimental results) to  $\alpha = 1/(1-2\nu)$  for pure plane-strain, where  $\nu$  is Poisson’s ratio. Considering

$$f = \frac{K_{op}}{K_{\max}} = \begin{cases} \max(R, A_0 + A_1R + A_2R^2 + A_3R^3), & R \geq 0 \\ A_0 + A_1R, & -2 \leq R < 0 \end{cases} \quad (11)$$

where the polynomial coefficients are given by:

$$\begin{cases} A_0 = (0.825 - 0.34\alpha + 0.05\alpha^2) \cdot [\cos(\pi\sigma_{\max}/2S_{fl})]^{1/\alpha} \\ A_1 = (0.415 - 0.071\alpha) \cdot \sigma_{\max}/S_{fl} \\ A_2 = 1 - A_0 - A_1 - A_3 \\ A_3 = 2A_0 + A_1 - 1 \end{cases} \quad (12)$$

Then, according to Newman, the effective stress intensity range  $\Delta K_{\text{eff}}$  can be expressed as:

$$\Delta K_{\text{eff}} = (1-f) \cdot K_{\max} = \frac{1-f}{1-R} \Delta K \quad (13)$$

DuQuesnay et al. [31] proposed crack closure models based on  $R$  and on the ratio between  $\sigma_{\max}$  and the cyclic yield strength  $S'_Y$ , however they did not explicitly account in their model for the stress-state dependence of crack closure. Figs. 3 and 4 show the influence of the

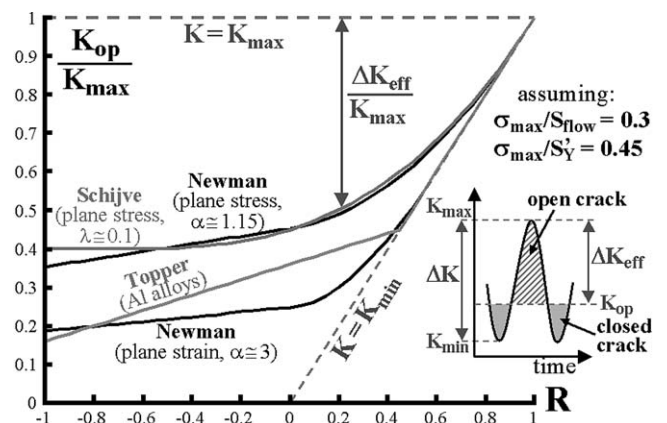


Fig. 3. Normalized opening SIF  $K_{op}/K_{\max}$  predictions as a function of the load ratio  $R$ .

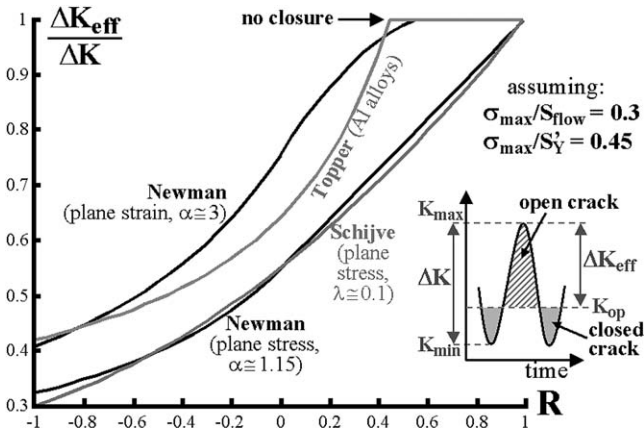


Fig. 4. Normalized effective stress intensity range predictions as a function of the load ratio.

load ratio  $R$  on  $K_{op}$  and on  $\Delta K_{eff}$ , as predicted by Newman, Schijve, and Topper–DuQuesnay.

Recently, Paris et al. [32] suggested that crack closure only occurs beyond a small distance  $d$  behind the crack tip, a phenomenon termed partial closure. Therefore, in an unloaded cracked body, the plastic strain wake around the crack faces would work as a wedge of thickness  $2h$  that would cause a non-zero stress intensity of (see Fig. 5):

$$K_{eff_{min}} = E'h/\sqrt{2\pi d} \tag{14}$$

where  $E' = E$  under plane–stress conditions or  $E' = E/(1-\nu^2)$  under plane–strain conditions, in which  $E$  is the Young’s modulus. To completely open the crack, releasing all compressive loads over the wedge, the crack opening displacement COD at a distance  $d$  of the crack tip must be equal to  $2h$ , therefore

$$\begin{aligned} COD &= \frac{4K_{op}}{E'} \sqrt{\frac{2d}{\pi}} = 2h \Rightarrow K_{eff_{min}} \\ &= \frac{E'}{\sqrt{2\pi d}} \frac{2K_{op}}{E'} \sqrt{\frac{2d}{\pi}} = \frac{2}{\pi} K_{op} \end{aligned} \tag{15}$$

and, assuming that  $K_{min} \leq 0$ , from Eq. (15) it can be concluded that

$$\Delta K_{eff} = K_{max} - (2/\pi)K_{op} \tag{16}$$

would be the actual effective stress intensity range under plasticity-induced crack closure conditions, a larger value than expected from Elber’s original model.

On the other hand, overload experiments in 2.25Cr1Mo steel have shown that crack closure is not the dominant crack retardation or arrest mechanism in plane–strain FCG, and cannot be used to justify the observed load sequence effects in these cases [33,34]. Moreover, other tests in the same steel have shown that there is FCG retardation and arrest after overloads but no crack closure at high  $R$ -ratios. Therefore, closure concepts again cannot be used to explain the observed interaction effects at such high  $R$ -ratios [34]. Lang and Marci [35] also found out that overload-induced crack closure does not occur at  $R > 0.5$ . They attribute the retardation phenomenon to the residual compressive stress field ahead of the crack tip after the overload. Another possible explanation could be due to crack path deflections and bifurcations [36], which can cause retardation due to the reduction in the SIF values caused by crack kinking. But what should be emphasized is that despite the crack closure concept popularity, it certainly cannot be used to justify the entire FCG behavior observed under VA loading.

Another category of crack closure models is based on Dugdale’s strip-yield model [37,38], adopted to calculate the plastic zone size and the associated residual plastic deformation. Plastic deformation is assumed to occur within thin strips of rigid perfectly-plastic material. Iterative solution procedures must be performed to calculate the amount of crack closure induced by all strips present in the plastic wake field. Several strip yield models have been proposed [24], however the non-linear nature of the material behavior makes them rather complex, often requiring measurements of several experimental constants that are very difficult to obtain.

There are several other FCG retardation models [17–19], but none of them has definitive advantages over the ones discussed above. As wisely recommended by Broek a long time ago [16], it probably can still be safely stated that, from an engineering point of view, retardation models should be calibrated by experimental data fitting. This is no surprise, since single equations are too simplistic to model all the several mechanisms that can induce retardation effects. Moreover, even  $da/dN \times \Delta K$  curves,

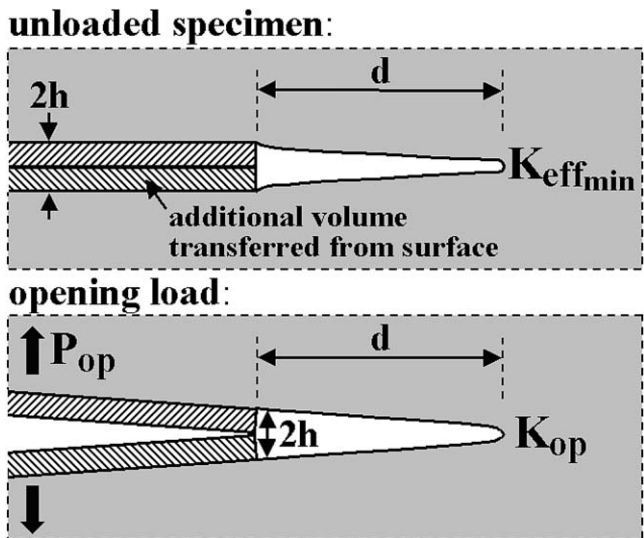


Fig. 5. Schematic of the partial closure model.

that are much simpler, still need to be measured for design purposes.

## 5. Crack propagation software

Two complementary pieces of software, named Quebra2D and ViDa [1,2,39], have been developed to implement the described two-step hybrid methodology. A brief description of both programs is presented below.

Quebra2D is an interactive graphical program for simulating 2D fracture processes based on a finite-element adaptive mesh-generation strategy [2,40]. This program includes all methods described above to compute the crack increment direction and the associated stress-intensity factors along the crack path. The crack representation scheme used in the Quebra2D program is based on the discrete approach, similar to well-known 2D simulators such as Franc2D [40]. However, Quebra2D brings some improvements with respect to its predecessors. It performs adaptive FE analyses, and its graphical interfaces are much more flexible, portable and friendly. Moreover, the adaptive FE analyses are coupled with modern and very efficient automatic remeshing schemes, which substantially decrease the required computational time.

The automatic calculation procedure in Quebra2D is performed in four steps: (i) the FE model of the cracked structure is solved to obtain (by the displacement correlation, by the modified crack closure or by the EDI methods [1–12])  $K_I$  and  $K_{II}$  and to calculate (by the  $\sigma_{\theta_{\max}}$ , by the  $G_{\theta_{\max}}$  or by the  $U_{\theta_{\min}}$  criteria [1,2,8,13–15]) the corresponding crack propagation direction; (ii) the crack is increased in the growth direction by a (small) specified step; (iii) the model is remeshed to account for the new crack size; and (iv) the process is iterated until rupture or until a specified crack size is reached. As a result, a list of  $K_I$  and  $K_{II}$  values is generated at relatively few intervals along the predicted crack paths.

The automatic meshing algorithm especially developed for Quebra2D works both for regions without cracks and for regions with one or multiple cracks, which may be either embedded or surface breaking. The 2D algorithm has been designed to meet four specific requirements, as follows: (i) it should produce well-shaped elements, avoiding elements with poor aspect ratio; (ii) the generated mesh should conform to an existing discretization on the region boundary; (iii) the algorithm should shift smoothly between regions with elements of highly varying size (because in crack analysis it is not uncommon for the elements near the crack tip to be two orders of magnitude smaller than the other elements); and (iv) the algorithm should have specific capabilities for modeling cracks, which are usually idealized without volume, i.e. the surfaces representing the

two sides of a crack face are distinct, but geometrically coincident. This means that nodes on opposite sides of crack faces may have identical coordinates, and the algorithm must be able to discriminate between them and to select the one on the proper crack side. Further details on the especially developed mesh generation algorithms can be found in Ref. [2].

The second program, named ViDa, is a general-purpose fatigue design program developed to predict both initiation and propagation fatigue lives under VA loading by all classical design methods, including the SN, the IIW (for welded structures) and the  $\epsilon N$  for crack initiation, and the  $da/dN$  for crack propagation [41]. It includes all load interaction models described above, predicting overload and underload-induced crack retardation and acceleration. This program does not require the global solution of the structure's stress field because it is based on the local approach, since its crack growth module is based on the direct integration of the fatigue crack propagation equation of the material,  $da/dN=F(\Delta K, R, \Delta K_{th}, K_C, \dots)$ , where  $\Delta K$  is the stress intensity range,  $R=K_{\min}/K_{\max}$  is the load ratio,  $\Delta K_{th}$  is the fatigue crack propagation threshold, and  $K_C$  is the fracture toughness of the structure. The program includes comprehensive database with hundreds of editable  $K_I$  and  $K_{II}$  SIF expressions and  $da/dN$  curves to be used in the calculations. In particular, ViDa accepts any crack growth equation and any SIF expression, making it an ideal companion to Quebra2D, which can be used to generate the required  $\Delta K$  expression if not available in its database.

The loading input in the ViDa software is sequential, and preserves the order information of the time signal that is lost when spectra, histograms or any other loading statistics are generated. To take advantage of this feature, a sequential rain-flow counting option has been introduced in that software. With this technique, the effect of each large loading event is counted when it happens, and not before its occurrence, as in the traditional rain-flow method, which could cause non-conservative predictions if overload effects are considered [1,2,39].

## 6. Experimental results

The FCG experiments were performed on 40 mm-wide 8 mm-thick compact tension C(T) test specimens, some of them modified with 7 mm-diameter holes specially positioned to curve the crack path. The specimens were made of a cold-rolled SAE 1020 steel plate with yield strength  $S_y = 285$  MPa, ultimate strength  $S_U = 491$  MPa, Young modulus  $E = 205$  GPa, and reduction in area  $RA = 54\%$ , measured according to the ASTM E 8M-99 standard, and with the analyzed weight percent composition given in Table 1.

The FCG tests were performed at two  $R$  ratios,  $R =$



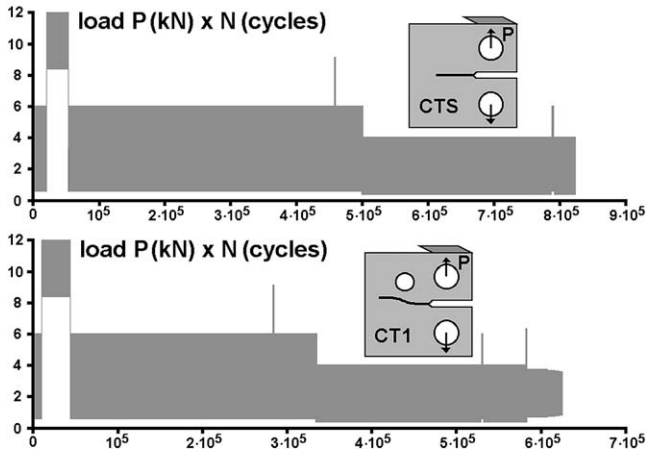


Fig. 9. Applied load history (in kN) for standard C(T) and modified CT1(VA) specimens.

around  $\Delta K_I \approx 20 \text{ MPa m}^{1/2}$  and load ratio  $R = 0.1$ . These loading values induce a stage-II (Paris regime) crack growth in the 1020 steel.

Two specimens were tested under VA loading: one standard C(T) specimen, and the holed specimen CT1(VA). The goals of this experiment were: (i) to check whether the curved crack paths predicted under CA loading would give good estimates of the measured paths under VA loading; and (ii) to verify whether load interaction models calibrated for straight cracks in the standard C(T) could be used to predict the fatigue life of the holed specimens, which present a curved crack path. The VA load histories applied to the tested specimens are shown in Fig. 9.

Fig. 10 shows the predicted and measured crack paths for the three modified specimens (in mm) under CA or VA loading, presenting a very good match. This suggests that the crack path under VA loading is the same as the one predicted under CA loading. Therefore, assuming

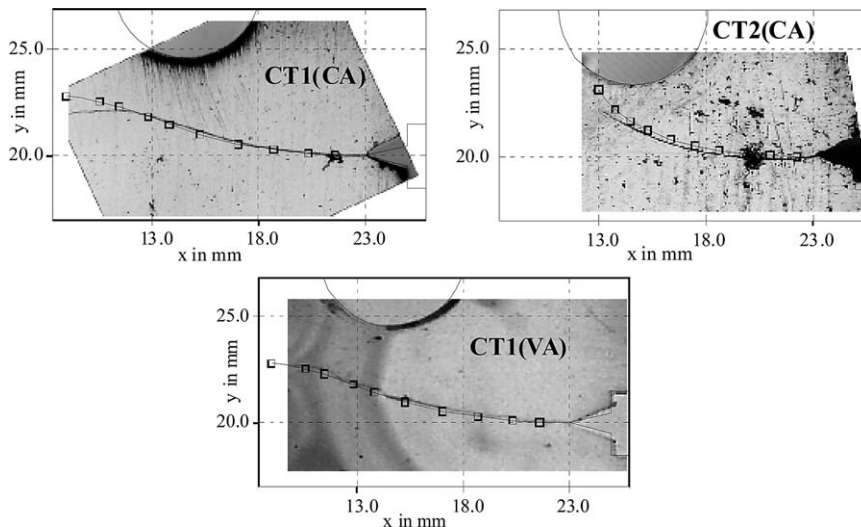


Fig. 10. Predicted and measured crack paths for the three modified C(T) specimens (mm).

that only the crack growth rate (but not its path) is influenced by load interaction effects, the discussed two-step methodology can be generalized to the VA loading case.

The SIF values calculated under CA loading along the crack path using the Quebra2D program were exported to the ViDa software to predict fatigue life, considering load interaction effects if necessary. Fig. 11 shows a very good match between predicted and measured crack sizes for the modified C(T) specimens under CA loading. The curved-crack predictions were based solely on crack growth data measured for straight-cracks and on SIF expressions calculated for the hole-modified specimens using FE.

To evaluate whether load interaction models calibrated from straight-crack experiments can be applied to specimens with curved cracks, several crack retardation models were calibrated (fitted) based on the standard C(T) data under VA loading. The better results were obtained by the Constant Closure model, where  $K_{op}$  was calibrated as 26% of the maximum overload SIF,  $K_{ol,max}$ ;

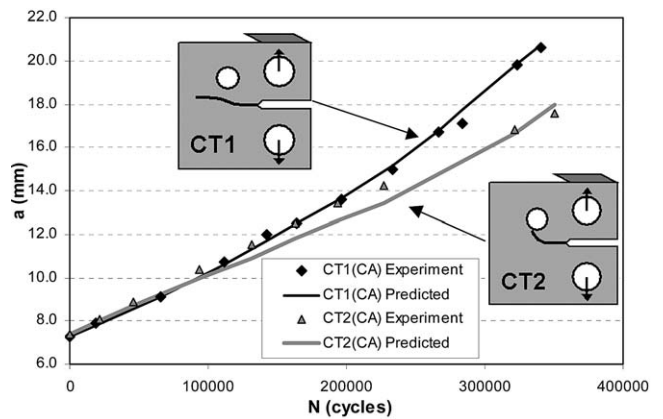


Fig. 11. Predicted and measured FCG for modified C(T) specimens under CA loading.

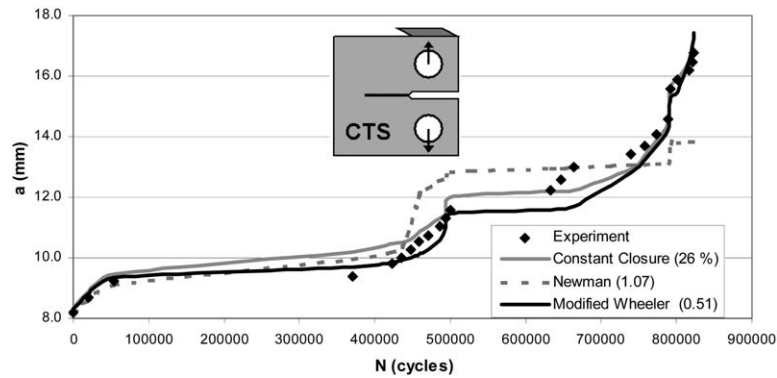


Fig. 12. Measured crack sizes and calibrated calculations on a standard C(T) under VA loading.

by the Modified Wheeler model, where the exponent  $\gamma$  was estimated as 0.51; and by Newman's closure model (generalized for the VA loading case), where the stress-state constraint was fitted as  $\alpha = 1.07$ , a value suggesting dominant plane-stress FCG conditions. The measured and fitted growth behavior is shown in Fig. 12.

The fitted load interaction parameters were then used to predict the crack growth behavior under VA loading of the hole-modified CT1(VA) specimen, see Fig. 13. The significant retardation effects of the CT1(VA) specimen were very well predicted using these three load interaction models in the ViDa program. In particular, the Modified Wheeler model results in very good predictions, possibly because its simplistic empirical yield-zone formulation can account for both closure and residual stress effects. These results suggest that load interaction models calibrated using straight cracks can be used to predict crack retardation behavior of curved cracks under VA loading.

However, it must be pointed out that the VA histories in Fig. 9 are very similar in nature, with similar stress levels and overload ratios. This similarity might be one of the reasons why the same load interaction model parameters could be used for both VA cases. The load-spectrum dependency of the crack retardation model parameters

might result in poor predictions if completely different VA histories are considered.

In addition, the very high sensitivity of the crack growth predictions with the load interaction model parameters is another error source that cannot be ignored. This sensitivity is particularly high when the crack growth rates approach stage I values, as seen in the post-overload regions with almost horizontal slope in Figs. 12 and 13. In this threshold region, miscalculations of just a few percent for the effective SIF can be the difference between crack growth or crack arrest. Since most life cycles are spent during stage I growth, this is the dominant (and most important) region in fatigue design, where the crack growth rates and load interaction effects should be better modeled and measured. This point must be carefully considered when analyzing in the literature crack retardation experiments performed under the Paris regime, where the high sensitivity of fatigue life with load interaction model parameters is masked by the smaller effect of crack closure or residual stress fields.

## 7. Conclusions

In this paper, a two-phase methodology to predict fatigue crack propagation in generic 2D structures was extended to VA loading histories, modeling crack retardation effects. First, self-adaptive FE were used to calculate the fatigue crack path and the SIF along the crack length, at each propagation step. The computed values were then used to predict the propagation fatigue life of the structure by the local approach, considering overload-induced crack retardation effects. Two complementary software products have been developed to implement this methodology. Experimental results validated the application of the proposed methodology to the VA loading case, suggesting that overloads do not significantly deviate the crack path predicted under CA loading. Moreover, the developed software could effectively predict the crack propagation path and fatigue life of an intricate 2D specimen under VA loading.

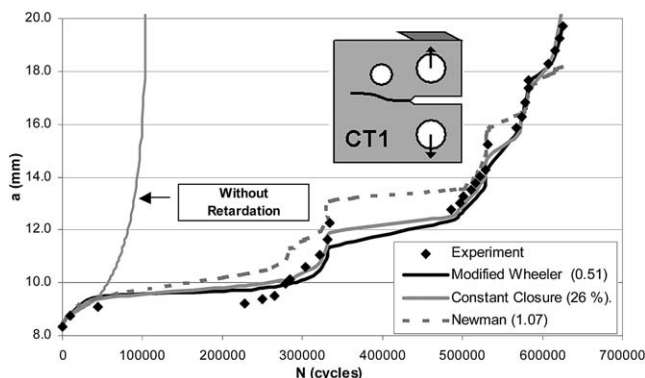


Fig. 13. Crack growth predictions (based on straight-crack calibrations) on a modified C(T) specimen under VA loading.

## Acknowledgements

We would like to thank Dr. Jorge Alberto Rodríguez Durán for obtaining most of the material properties for the SAE 1020 steel used in this study, and to CAPES and CNPq for scholarships that partially supported this research.

## References

- [1] Miranda ACO, Meggiolaro MA, Castro JTP, Martha LF, Bittencourt TN. Fatigue crack propagation under complex loading in arbitrary 2D geometries. In: Braun AA, McKeighan PC, Lohr RD, editors. Applications of automation technology in fatigue and fracture testing and analysis. ASTM STP. 2002. p. 120–45.
- [2] Miranda ACO, Meggiolaro MA, Castro JTP, Martha LF, Bittencourt TN. Fatigue life and crack path prediction in generic 2D structural components. *Eng Fract Mech* 2003;70(10):1259–79.
- [3] Shih CF, de Lorenzi HG, German MD. Crack extension modeling with singular quadratic isoparametric elements. *Int J Fract* 1976;12:647–51.
- [4] Rybicki EF, Kanninen MF. A finite element calculation of stress-intensity factors by a modified crack closure integral. *Eng Fract Mech* 1977;9:931–8.
- [5] Raju IS. Calculation of strain-energy release rates with higher order and singular finite elements. *Eng Fract Mech* 1987;28:251–74.
- [6] Nikishkov GP, Atluri SN. Calculation of fracture mechanics parameters for an arbitrary three-dimensional crack by the equivalent domain integral method. *Int J Numer Methods Eng* 1987;24:1801–21.
- [7] Dodds Jr. RH, Vargas PM. Numerical evaluation of domain and contour integrals for nonlinear fracture mechanics. Urbana, Champaign: Department of Civil Engineering, University of Illinois; 1988.
- [8] Bittencourt TN, Wawrzynek PA, Ingraffea AR, Sousa JLA. Quasi-automatic simulation of crack propagation for 2D LEFM problems. *Eng Fract Mech* 1996;55:321–34.
- [9] Rice JR. A path independent integral and the approximate analysis of strain concentration by notches and cracks. *J Appl Mech* 1968;35:379–86.
- [10] Knowles JK, Sternberg E. On a class of conservation laws in linearized and finite elastostatics. *Arch Rational Mech Anal* 1972;44:187–211.
- [11] Atluri SN. Path-independent integrals in finite elasticity and inelasticity, with body forces, inertia, and arbitrary crack-face conditions. *Eng Fract Mech* 1982;16:341–64.
- [12] Bui HD. Associated path independent  $J$ -integrals for separating mixed modes. *J Mech Phys Solids* 1983;31:439–48.
- [13] Erdogan F, Sih GC. On the crack extension in plates under plane loading and transverse shear. *J Basic Eng* 1963;85:519–27.
- [14] Hussain MA, Pu SU, Underwood J. Strain energy release rate for a crack under combined Mode I and II. ASTM STP 560. 1974. p. 2–28.
- [15] Sih GC. Strain-energy-density factor applied to mixed mode crack problems. *Int J Fract Mech* 1974;10:305–21.
- [16] Broek D. The practical use of fracture mechanics. Kluwer; 1988.
- [17] Suresh S. Fatigue of materials. Cambridge University Press; 1998.
- [18] Skorupa M. Load interaction effects during fatigue crack growth under variable amplitude loading—a literature review, Part 1: empirical trends. *Fatigue Fract Eng Mater Struct* 1998;21:987–1006.
- [19] Skorupa M. Load interaction effects during fatigue crack growth under variable amplitude loading—a literature review, Part 2: qualitative interpretation. *Fatigue Fract Eng Mater Struct* 1999;22:905–26.
- [20] Sadananda K, Vasudevan AK, Holtz RL, Lee EU. Analysis of overload effects and related phenomena. *Int J Fatigue* 1999;21:S233–S46.
- [21] Meggiolaro MA, Castro JTP. An evaluation of Elber-type crack retardation models. II SAE-Brazil International Fatigue Seminar. 2001. p. 207–16 SAE #2001-01-4063, SAE.
- [22] Elber W. The significance of fatigue crack closure. ASTM STP 486. 1971.
- [23] von Euw EFG, Hertzberg RW, Roberts R. Delay effects in fatigue crack propagation. In: ASTM STP 513. 1972. p. 230–59.
- [24] Schijve J. Fatigue of structures and materials. Kluwer Academic Publishers; 2001.
- [25] de Koning AU, ten Hoeve HJ, Hendriksen TK. The description of crack growth on the basis of the strip-yield model for computation of crack opening loads, the crack tip stretch and strain rates. National Aerospace Lab. (NLR), Report NLR-TP-97511L, 1997.
- [26] Wheeler OE. Spectrum loading and crack growth. *J Basic Eng* 1972;181–6.
- [27] Willenborg J, Engle RM, Wood HA. Crack growth retardation model using an effective stress concept. Air Force Flight Dynamics Laboratory, Wright Patterson Air Force Base, TM 71-1-FBR, 1971.
- [28] Bunch JO, Trammell RT, Tanouye PA. Structural life analysis methods used on the B-2 bomber. Advances in fatigue lifetime predictive techniques. ASTM 1996;3:220–47 [A96-26758 06-39].
- [29] Schijve J. The stress ratio effect on fatigue crack growth in 2024-T3 Alclad and the relation to crack closure. Technische Hogeschool Delft, Memorandum M-336, 1979.
- [30] Newman Jr JC. A crack opening stress equation for fatigue crack growth. *Int J Fract* 1984;24(3):R131–R5.
- [31] DuQuesnay DL, Topper TH, Yu MT, Pompetzki MA. The effective stress range as a mean stress parameter. *Int J Fatigue* 1992;14(1):45–50.
- [32] Paris PC, Tada H, Donald JK. Service load fatigue damage—a historical perspective. *Int J Fatigue* 1999;21:S35–S46.
- [33] Castro JTP, Parks DM. Decrease in closure and delay of fatigue crack growth in plane strain. *Scripta Metall* 1982;16:1443–5.
- [34] Meggiolaro MA, Castro JTP. On the dominant role of crack closure on fatigue crack growth modeling. *Int J Fatigue*, in press [doi: 10.1016/S0142-1123(03)00132-4].
- [35] Lang M, Marci G. The influence of single and multiple overloads on fatigue crack propagation. *Fatigue Fract Eng Mater Struct* 1999;22:257–71.
- [36] Suresh S. Micromechanisms of fatigue crack growth retardation following overloads. *Eng Fract Mech* 1983;18:577–93.
- [37] Dugdale DS. Yielding of steel sheets containing slits. *J Mech Phys Solids* 1960;8:100–4.
- [38] Fühling H, Seeger T. Dugdale crack closure analysis of fatigue cracks under constant amplitude loading. *Eng Fract Mech* 1979;11(1):99–122.
- [39] Meggiolaro MA, Castro JTP. ViDa—a visual damagemeter to automate the fatigue design under complex loading. *J Braz Soc Mech Sci* 1998;20:666–85 (in Portuguese).
- [40] Wawrzynek PA, Ingraffea AR. Interactive finite element analysis of fracture processes: an integrated approach. *Theor Appl Fract Mech* 1987;8:137–50.
- [41] Homepage. Available from: <http://www.tecgraf.puc-rio.br/vida>.